DALTON
FULL PAPER

Synthesis, structure and density functional study of the *ansa*-rhenocene complex [Re{(η-C_5H_4)CMe_2(η-C_5H_4)}Cl] †

Stephen L. J. Conway, Linda H. Doerrer, Jennifer C. Green,* Malcolm L. H. Green, Adrian Scottow and Adam H. H. Stephens

Inorganic Chemistry Laboratory, South Parks Road, Oxford, UK OX1 3QR.
E-mail: malcolm.green@chem.ox.ac.uk

Received 29th October 1999, Accepted 3rd December 1999

The *ansa*-rhenocene compound [Re{(η-C_5H_4)CMe_2(η-C_5H_4)}Cl] **1** has been prepared by reaction of $ReCl_5$ with [K_2(C_5H_4)CMe_2(C_5H_4)]. X-Ray crystallography shows the molecular structure to be unsymmetrical, with the angle defined by the Re-bridgehead carbon vector and the chlorine atom found to be 170.4°. A density functional study compares the electronic structure of [Re{(η-C_5H_4)CH_2(η-C_5H_4)}Cl] with [Re{(η-C_5H_5)$_2$Cl] and shows that for the *ansa*-bridged species, the chlorine binds less effectively in the central position. The calculated structure of [Re{(η-C_5H_4)CH_2(η-C_5H_4)}Cl] is also found to be unsymmetrical.

Introduction

Recently, we have described *ansa*-metallocenes of Group 6 metals and shown differences in structure and reactivity to the well-defined non-bridged analogues.[1–3] The influence on structure and reactivity is found to be most marked when the cyclopentadienyl ligands are bridged by one carbon atom. For instance, thermolysis of [W(η-C_5H_5)$_2$Me(H)] results in reductive elimination of methane above 48 °C, whereas the carbon bridged analogue [W{(η-C_5H_4)CMe_2(η-C_5H_4)}Me(H)] is stable up to 120 °C. Reductive elimination from [W(η-C_5H_5)$_2$$X_2$] species has been shown to generate the 16-electron intermediate [W(η-C_5H_5)$_2$]. This intermediate adopts a ground state structure in which the cyclopentadienyl rings are parallel.[4] The increased stability of the *ansa*-bridged compound was attributed to the inability of [W{(η-C_5H_4)CMe_2(η-C_5H_4)}] to adopt a parallel ring structure.[1] A recent detailed density functional study supports this assertion.[5]

The cationic rhenocene alkyl hydrides [Re(η-C_5H_5)$_2$R(H)]$^+$ are highly labile, undergoing alkane elimination, even at low temperatures.[6,7] Since the fragments [W(η-C_5H_5)$_2$] and [Re(η-C_5H_5)$_2$]$^+$ are isoelectronic, it is anticipated that the stability of rhenocene alkyl hydrides might be increased by the presence of a single carbon *ansa*-bridge.

During the course of this work Heinekey and Radzewich have described the first *ansa*-rhenocene compounds and preliminary investigations have shown that the silicon-bridged species [Re{(η-C_5H_4)$SiMe_2$(η-C_5H_4)}Me(H)]$^+$ displays increased thermal stability relative to the non-bridged analogue.[8] The possibility of greater stabilisation when constraining the cyclopentadienyl rings further by bridging with a CR_2 unit is also discussed, although synthetic efforts were unsuccessful.

Here we describe an entry into carbon-bridged *ansa*-rhenocene chemistry with the synthesis and characterisation of [Re{(η-C_5H_4)CMe_2(η-C_5H_4)}Cl]. The molecular structure and a density functional study of the compound illustrate the effect of the presence of an *ansa*-bridge on the orbital structure of bent metallocenes.

† Electronic supplementary information (ESI) available: rotatable 3-D structure in CHIME format. See http://www.rsc.org/suppdata/dt/a9/a908619f/

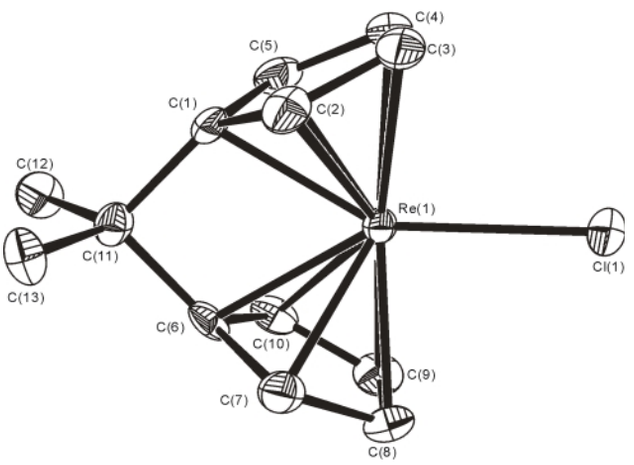

Fig. 1 Molecular structure of [Re{(η-C_5H_4)CMe_2(η-C_5H_4)}Cl] **1**. Hydrogen atoms attached to carbon atoms are omitted for clarity.

Results and discussion

Synthesis

A procedure analogous to that described for the synthesis of the non-bridged rhenocene [Re(η-C_5H_5)$_2$Cl][9] was used to prepare the compound [Re{(η-C_5H_4)CMe_2(η-C_5H_4)}Cl] **1**. Addition of excess [K_2(C_5H_4)CMe_2(C_5H_4)] to $ReCl_5$ in dme at low temperature followed by extraction into thf and then dichloromethane gives crude **1** as a red–brown solid in 10% yield. An analytically pure sample of **1** was obtained by recrystallisation from a dichloromethane solution in a final yield of *ca.* 3%.

The ^{1}H NMR spectrum of **1** consists of two partial triplets (δ 5.43 and 4.28) corresponding to the two sets of cyclopentadienyl protons and a singlet (δ 1.03) due to the protons of the CMe_2 bridge. Compound **1** was also characterised by ^{13}C{^{1}H} NMR spectroscopy, FAB (fast atom bombardment) mass spectrometry and X-ray crystallography.

The molecular structure of **1** was determined and its molecular structure, with atomic numbering scheme, is shown in Fig. 1. The geometrical parameters relevant to *ansa*-metallocenes are defined in Fig. 2. Selected interatomic distances and angles for the compound **1** are given in Table 1. The bending angles β and γ are 126.9 and 131.3°, respectively. These angles are

Table 1 Selected interatomic distances (Å) and angles (°) for [Re{(η-C_5H_4)CMe_2(η-C_5H_4)}Cl] **1**

Re–Cl	2.4383(13)	Re–C(1)	2.175(5)
Re–C(2)	2.218(5)	Re–C(3)	2.245(5)
Re–C(4)	2.245(5)	Re–C(5)	2.199(5)
Re–C(11)	2.8912	Re–Cp_{cent} (av.)	1.855
C(1)–C(2)	1.454(7)	C(2)–C(3)	1.398(8)
C(3)–C(4)	1.439(9)	C(4)–C(5)	1.416(8)
C(1)–C(5)	1.448(7)		
C(1)–C(11)–C(6), ε	195.8(4)	Angle between Cp planes, α	1.912
Cp^1_{norm}–Re–Cp^2_{norm}, β	126.9	Cp^1_{cent}–Re–Cp^2_{cent}, γ	131.3
Cp_{ipso}–Cp plane, φ	20.9, 22.0	(C11)···Re–Cl, θ	170.44

(Cp^1 = Ring C(1)–C(5), Cp^2 = Ring C(6)–C(10).

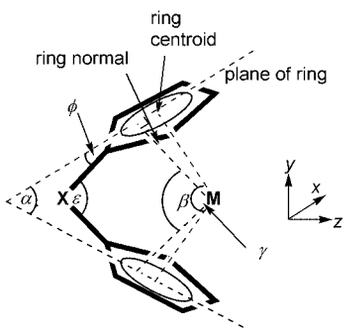

Fig. 2 Geometric parameters in an *ansa*-metallocene. α = angle between the ring planes; β = angle between the normals from the metal to the ring planes; γ = ring centroid–metal–ring centroid angle; ε = angle between vectors from a bridging atom X to the *ipso*-carbons; φ = angle between *ipso*-carbon vector and the ring plane.

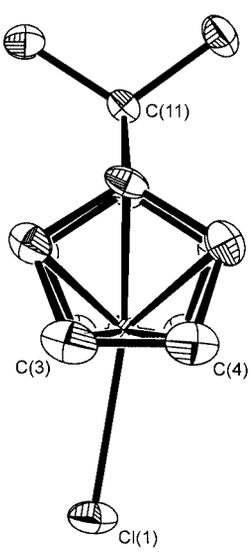

Fig. 3 Alternative view of the molecular structure of [Re{(η-C_5H_4)-CMe_2(η-C_5H_4)}Cl] **1**.

much reduced compared to the non-bridged analogue [Re(η-C_5H_5)$_2$Cl][9] (γ = 147.6°) and suggest a greater strain is imparted by the CMe_2 bridge. The bending angle γ in the silicon-bridged species [Re{(η-C_5H_4)$SiMe_2$(η-C_5H_4)}Me][8] (γ = 145.2°) is close to that found in non-bridged species. The CMe_2 bridge imposes a significant distortion from planarity at the *ipso*-carbon (φ = 20.9 and 22.0°). The Re–C(1) and Re–C(6) distances are the shortest Re–C interactions, suggesting that the bonding mode of the η-cyclopentadienyl rings is partially η^3 in character.

Of particular note in the molecular structure is the angle θ, defined by the C(11)···Re vector and the chlorine atom, which is found to have a value of 170.4° (Fig. 3). This phenomenon is not seen in other rhenocene derivatives. For instance, in the non-bridged analogue [Re(η-C_5H_5)$_2$Cl] where the rings are slightly staggered, a point X can be defined at the centroid of the four carbon atoms furthest from Cl. The angle X···Re–Cl is found to be 179.4°. As a result of the Re–Cl bond being displaced from the C(11)···Re vector in **1**, the rings are slightly canted with the side to which the chlorine atom lies becoming more open. The C(2)–C(7) distance is 0.194 Å longer than the C(5)–C(10) and the C(3)–C(8) distances and 0.106 Å longer than the C(4)–C(9) distance.

The low yield of **1** is not unexpected in the light of our experience in the synthesis of Group 6 *ansa*-metallocenes[2,3] and the low yielding synthesis of non-bridged rhenocene complexes.[7,9] Heinekey and Radzewich described the synthesis of [Re{(η-C_5H_4)$SiMe_2$(η-C_5H_4)}Me] in high yield *via* the deprotonation of [Re(η^5-C_5H_5)$_2$Me], followed by reaction with Me_2SiCl_2.[8] This route was not successful for the preparation of carbon-bridged *ansa*-rhenocene complexes.

Electronic structure of [Re{(η-C_5H_4)CH_2(η-C_5H_4)}Cl]

Previous experience with theoretical prediction of properties of *ansa*-bridged compounds using density functional theory[5,10–12] suggested that an explanation for the structure of **1** might emerge from a similar study here. In particular, it has been noted previously[5,12] that with a single carbon-bridge between the two rings, binding to the *ipso*-carbons is strengthened at the expense of a centrally bound additional ligand, such as the central H on a metallocene trihydride.[12] It seemed likely that similar factors might be responsible for the structure of **1**.

In order to understand the origin of the unsymmetrical structure of **1** we carried out density functional calculations on [Re{(η-C_5H_4)CH_2(η-C_5H_4)}Cl] **I** as a model for **1** and the unbridged analogue [Re(η-C_5H_5)$_2$Cl] **II**. Geometry optimisations on **I** and **II** resulted in the bond lengths, interatomic distances and angles given in Table 2. The calculations gave a structure with C_{2v} symmetry for **II** but the lowest energy geometry found for **I** had an angle of 175.6° between the Re–Cl bond and the Re···C(11) vector. This is somewhat larger than that found experimentally for **1**, but was consistently reproduced from a number of different starting geometries. Frequency calculations on the optimised structures gave only positive frequencies for **II** but for **I** an imaginary frequency of 40i cm^{-1} was found, corresponding to a wagging of the Cl in the *xz* plane. The structure was re-optimised including the gradient corrections in the SCF convergence. Studies on a number of transition metal carbonyl complexes have shown this procedure to give longer distances in closer agreement with experiment.[13] In this case distances (also given in Table 2) were found to be longer, but in less good agreement with experiment, and a C(11)···Re–Cl angle of 165.5° was the result. A frequency calculation on this structure gave all real frequencies, confirming that a local minimum had been identified. The Cl wag was the lowest energy vibration, with a wavenumber of 40 cm^{-1}. It is evident that the Cl wag in the *xz* plane is a very low energy vibration.

For comparative purposes the geometry of **I** was also optimised with C_{2v} symmetry. Molecular orbital (MO) schemes for **I** and **II**, with C_{2v} symmetry, are given in Fig. 4 together with the orbital energy levels for the corresponding fragments, [Re{(η-C_5H_4)CH_2(η-C_5H_4)}] and [Re(η-C_5H_5)$_2$], also with C_{2v} symmetry. The fragment calculations are performed on the same geometry as that found in the molecular optimised structure. There are marked differences in the two molecular energy schemes, notably the b_1 HOMO (highest occupied molecular orbital) is of higher energy in **I** than **II**, whereas the a_1 HOMO-1 is significantly more stable in **I** than **II**. Representations of these orbitals are shown in Fig. 5(a) and 5(c). The relative energies of the HOMO and HOMO-1, and other

Table 2 Calculated bond lengths (Å) and angles (°) for [Re{(η-C_5H_4)CH_2(η-C_5H_4)}Cl] **I** and [Re(η-C_5H_5)$_2$Cl] **II**

	I (calc.)[a]	**I** (calc.)[b]	**1**	**II** (calc.)	**II** (exp.)
Re–Cl	2.479	2.433	2.4383(13)	2.461	2.438(3)
Re–C(1)	2.234	2.208	2.175(5)	2.217	2.210(20)
Re–C(2)	2.302	2.243	2.218(5)	2.217	2.220(10)
Re–C(3)	2.340	2.290	2.245(5)	2.292	2.286(9)
Re–C(4)	2.343	2.287	2.245(5)	2.292	2.280(10)
Re–C(5)	2.250	2.225	2.199(5)	2.302	2.230(10)
Re–C(11)	2.885	2.864	2.8912		
Re–Cp_{cent} (av.)	1.939	1.893	1.855	1.912	1.886
C(1)–C(2)	1.456	1.446	1.454(7)	1.436	1.400(20)
C(2)–C(3)	1.420	1.412	1.398(8)	1.427	1.410(20)
C(3)–C(4)	1.450	1.443	1.439(9)	1.420	1.440(20)
C(4)–C(5)	1.429	1.415	1.416(8)	1.420	1.380(20)
C(1)–C(5)	1.460	1.447	1.448(7)	1.427	1.400(20)
θ	165.6	175.4	170.44	180.0[c]	179.4[c]
α	57.0	55.2	53.1	36.5	40.2
β	123.0	124.8	126.9	143.5	139.8
φ	21.8	22.0	20.9, 22.0		
ε	99.9	99.2	95.8		
γ	130.0	130.0	131.3	149.6	147.6

[a] Non-local correction included throughout the calculation. [b] Non-local correction not used in calculating gradients. [c] For **II**: θ defined as X · · · Re–Cl where X is the centroid of the four η-cyclopentadienyl carbon atoms furthest from Cl.

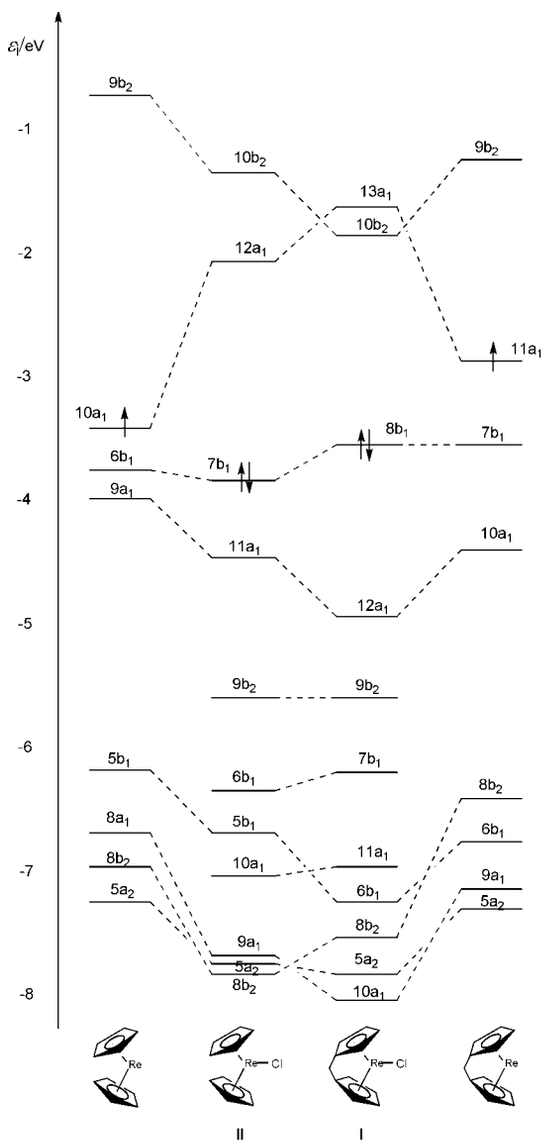

Fig. 4 MO schemes for the fragment [Re(η-C_5H_5)$_2$], [Re(η-C_5H_5)$_2$Cl] **II**, [Re{(η-C_5H_4)CH_2(η-C_5H_4)}Cl] **I** and the fragment [Re{(η-C_5H_4)-CH_2(η-C_5H_4)}]. Dashed lines correlate related orbitals. The levels in the schemes for **I** and **II** which are not correlated with fragment orbitals are principally chloride 3p in origin.

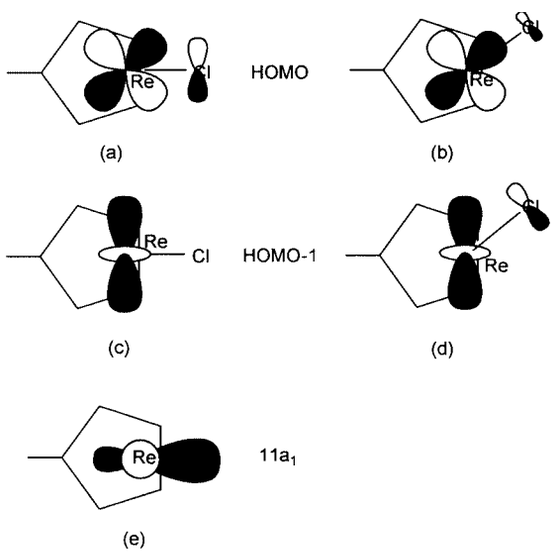

Fig. 5 Representations of selected orbitals. HOMO of **I** when: (a) $\theta = 180°$; (b) $\theta < 180°$. HOMO-1 of **I** when (c) $\theta = 180°$; (d) $\theta < 180°$. (e) $11a_1$ orbital of the fragment [Re{(η-C_5H_4)CH_2(η-C_5H_4)}].

energy differences in the metal cyclopentadienyl bonding orbitals, may be traced back to energy differences between the two parent fragments. The larger inter-ring angle, α, in the *ansa*-bridged analogue leads to a greater energy spread of the three frontier metal orbitals.[5] In the fragments, in addition to the differences in the lower a_1 and b_1 orbitals already noted, an upper a_1 orbital ($11a_1$) is significantly raised in energy in the fragment [Re{(η-C_5H_4)CH_2(η-C_5H_4)}] compared with the analogous orbital ($10a_1$) in the fragment [Re(η-C_5H_5)$_2$]. The former, shown in Fig. 5(e), is the orbital available to bind a group in the central position. Thus, it may be anticipated that it will be less effective in covalent bonding when the rings are linked by an *ansa*-bridge. Population analysis shows that in **I** the $11a_1$ fragment orbital has an occupancy of 0.37 electrons and the Cl $3p_z$ orbital 1.61 electrons, whereas in **II** the corresponding fragment $10a_1$ orbital has an occupancy of 0.46 electrons and the Cl $3p_z$ orbital 1.55 electrons. Thus, we may conclude that bonding in the central position is less favoured by the introduction of an *ansa*-bridge.

Geometry optimisation of the analogous *ansa*-bridged hydride [Re{(η-C_5H_4)CH_2(η-C_5H_4)}H] gave a structure with

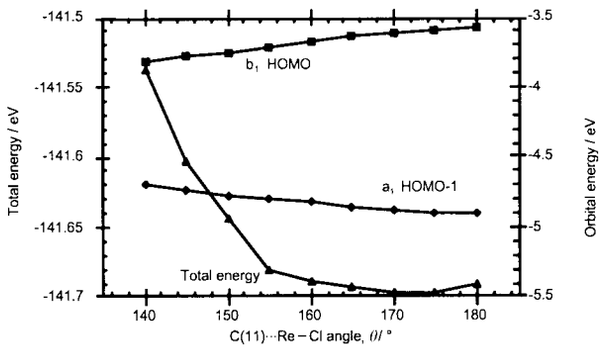

Fig. 6 Plot of the variation of the total energy, the energy of the HOMO and the HOMO-1 of [Re{(η-C_5H_4)CH_2(η-C_5H_4)}Cl] **I**, with the C(11)···Re–Cl angle, θ.

C_{2v} symmetry and a C(11)···Re–H angle of 180°, which suggests that the pπ electrons of the Cl might well be responsible for the distortion.

Further analysis was undertaken with a linear transit calculation on **I** in which the C(11)···Re–Cl angle, θ, was varied between 140 and 180° and the remainder of the molecule was geometry optimised. The energy variations with angle obtained for the molecule and the upper orbitals are shown in Fig. 6. This confirms the presence of a very shallow minimum in the energy surface at a C(11)···Re–Cl angle of around 175° and shows that as θ decreases, the energy of the HOMO drops and that of the HOMO-1 rises. The reason for these changes is evident from the nodal properties of these two orbitals, shown in Fig. 5. The HOMO is largely metal in character but metal–Cl pπ antibonding [Fig. 5(a)]. Moving the Cl off the central position relieves the anti-bonding interaction [Fig. 5(b)]. The HOMO-1 is, by contrast, metal–Cl non-bonding when the Cl is centrally placed [Fig. 5(c)], but becomes anti-bonding as the Cl is moved to one side [Fig. 5(d)]. It appears to be this interaction which favours a small displacement of the Cl. That it does not also occur in the unbridged compound is due to the fact that the σ-bonding of the halide is more directed in this case.

Experimental

General

All manipulations of air- and/or moisture-sensitive materials were performed in an inert atmosphere using either a dual vacuum–nitrogen line and standard Schlenk techniques, or in an inert atmosphere dry box containing nitrogen. In each case, the nitrogen was purified by passage over 4 Å molecular sieves and either BASF catalyst for the dry box, or MnO for the Schlenk line. Solvents and solutions were transferred through stainless steel cannulae using a positive pressure of nitrogen. Filtrations were generally performed using modified stainless steel cannulae which had been fitted with glass fibre filter discs. All glassware and cannulae were dried overnight at 150 °C before use.

Physical measurements

The ^{1}H and ^{13}C NMR spectra were recorded using a Varian UNITY *plus* (^{1}H 500 MHz, ^{13}C 125 MHz) spectrometer at room temperature. Spectra were referenced internally using the residual protio solvent (^{1}H) and solvent (^{13}C) resonances relative to tetramethylsilane (δ 0). Mass spectra (FAB) were performed by the EPSRC Mass Spectrometry Service at Swansea. Elemental analyses were performed by the Microanalytical Department of the Inorganic Chemistry Laboratory, Oxford.

Materials

Solvents were pre-dried by standing over 4 Å molecular sieves and then refluxed and distilled under a nitrogen atmosphere from calcium hydride (dichloromethane) or sodium–potassium alloy (1 : 3 w/w) (dme, thf). Deuterated solvents (Aldrich) for NMR studies were dried by refluxing with calcium hydride, distilled and stored under nitrogen in Young's tap ampoules. $ReCl_5$[14] and [K_2(C_5H_4)CMe_2(C_5H_4)][15,16] were prepared *via* literature methods.

Synthesis

[Re{(η-C_5H_4)CMe_2(η-C_5H_4)}Cl] 1. A suspension of [K_2-(C_5H_4)CMe_2(C_5H_4)] (3.36 g, 13.52 mmol) in dme (30 cm^3) at −78 °C was added to a stirred suspension of $ReCl_5$ (1.64 g, 4.51 mmol) at −78 °C in dme (50 cm^3). The dark red reaction mixture was allowed to slowly warm to room temperature and stirred overnight. The reaction mixture was filtered and volatiles removed under reduced pressure. The resulting dark brown oily solid was extracted into thf (2 × 30 cm^3) to give a dark brown solution. The solvent was removed under reduced pressure and the resulting solid was extracted into dichloromethane (30 cm^3) to give a dark red solution. Removal of volatiles under reduced pressure yielded crude [Re{(η-C_5H_4)CMe_2(η-C_5H_4)}Cl] **1** as a red–brown solid. Yield (based on $ReCl_5$) 0.17 g, 9.6%. An analytically pure sample of **1** was obtained by as a red–orange crystalline solid by recrystallisation from a dichloromethane solution at −80 °C. Final yield 0.06 g, 3.4%. ^{1}H NMR [500 MHz, $(CD_3)_2CO$]: δ 5.43 (m, 4H, C_5H_4), 4.28 (m, 4H, C_5H_4), 1.03 (s, 6H, CMe_2). ^{13}C{^{1}H} NMR [125 MHz, $(CD_3)_2CO$]: δ 83.12 (s, C_5H_4), 75.78 (s, C_5H_4), 34.393 (s, C_{ipso} or CMe_2), 30.99 (s, C_{ipso} or CMe_2), 21.66 (s, CMe_2). FAB-MS: *m*/*z* 392 (M^+), 357 (M^+ − Cl). Anal. calcd for $C_{13}H_{14}ReCl$: C, 39.8; H, 3.6; found: C, 39.75; H, 3.93%.

Crystallography

Red–orange crystals of the compound **1** were grown from a dichloromethane solution at *ca.* 193 K and isolated by filtration. A specimen was chosen under an inert atomsphere, covered with paratone-N oil, and mounted on the end of a glass fibre.

Data were collected at 150 K on an Enraf-Nonius DIP2000 image plate diffractometer with graphite-monochromated Mo-Kα radiation (λ = 0.71069 Å). The images were processed with the DENZO[17] and SCALEPACK programs.[18] Corrections for Lorentz and polarisation effects were performed.

All solution, refinement and graphical calculations were performed using the CRYSTALS[19] and CAMERON[20] software packages. The crystal structure was solved by direct methods using the SIR92 program[21] and was refined by full-matrix least squares procedures on *F*. All non-hydrogen atoms were refined with anisotropic displacement parameters. All carbon-bound hydrogen atoms were generated and allowed to ride on their corresponding carbon atoms with fixed thermal parameters. A Chebychev weighting scheme with the parameters 1.59, 0.554 and 1.16 was applied, as well as an empirical absorption correction.[22]

The crystallographic and refinement data are summarised in Table 3.

CCDC reference number 186/1765.

See http://www.rsc.org/suppdata/dt/a9/a908619f/ for crystallographic files in .cif format.

Computational details

Calculations were performed using the density functional methods of the Amsterdam Density Function package (Version 2.3).[23] The electronic configurations were described by an uncontracted triple-ζ basis set of Slater-type orbitals, with a single polarisation function added; 2p on hydrogen, 3d on carbon and 4d on chlorine atoms. The cores of the atoms were frozen, carbon up to the 1s, chlorine to the 2p and rhenium to the 5p. First order relativistic corrections were made to the

Table 3 Crystallographic and refinement data for [Re{(η-C_5H_4)CMe_2-(η-C_5H_4)}Cl] **1**

Formula	$C_{13}H_{14}ClRe$
FW	391.91
Crystal system	Monoclinic
Space group	$P\,2_1/n$
Crystal dimensions/mm	0.25 × 0.25 × 0.20
a/Å	7.125(5)
b/Å	11.794(4)
c/Å	13.524(8)
β/°	103.08(3)
V/Å^3	1107.0
Z	4
ρ_{calc}/g cm^{-3}	2.35
T/K	150
μ(Mo-Kα)/mm^{-1}	1.133
Total no. of data	3662
No. of unique data	2238
No. of observed data [a]	1953
No. of parameters	136
R_{int}	0.08
R [b]	0.035
R_W [b]	0.040

[a] Criterion for observation $I > 3\sigma(I)$. [b] $R = [\Sigma(|F_o| - |F_c|)/\Sigma|F_o|]$ $Rw = [\Sigma w(F_o^2 - F_c^2)^2/\Sigma w(F_o^2)^2]^{1/2}$.

cores of all atoms using the Pauli formalism. Energies were calculated using Vosko, Wilk and Nusair's local exchange correlation,[24] with non-local-exchange corrections by Becke,[25] and non-local correlation corrections by Perdew.[26] In general the non-local correction terms were not utilised in calculating gradients during geometry optimisations. In the case of **I**, optimisation was also carried out including the non-local corrections throughout the calculation.

Acknowledgements

We are grateful for Junior Research Fellowships to Lincoln College, Oxford (to A. H. H. S.) and St. John's College, Oxford (to L. H. D.) and the EPSRC for a studentship (to S. L. J. C.). We are also grateful to Dr Leigh H. Rees for assistance with X-ray crystallography.

References

1 L. Labella, A. Chernega and M. L. H. Green, *J. Chem. Soc.*, *Dalton Trans.*, 1995, 395.
2 A. Chernega, J. Cook, M. L. H. Green, L. Labella, S. J. Simpson, J. Souter and A. H. H. Stephens, *J. Chem. Soc.*, *Dalton Trans.*, 1997, 3225.
3 S. L. J. Conway, T. Dijkstra, L. H. Doerrer, J. C. Green, M. L. H. Green and A. H. H. Stephens, *J. Chem. Soc.*, *Dalton Trans.*, 1998, 2689.
4 N. J. Cooper, M. L. H. Green and R. Mahtab, *J. Chem. Soc.*, *Dalton Trans.*, 1979, 1557.
5 J. C. Green, *Chem. Soc. Rev.*, 1998, **27**, 263.
6 D. M. Heinekey and G. L. Gould, *J. Am. Chem. Soc.*, 1989, **111**, 5502.
7 D. M. Heinekey and G. L. Gould, *Organometallics*, 1991, **10**, 2977.
8 D. M. Heinekey and C. E. Radzewich, *Organometallics*, 1999, **18**, 3070.
9 C. Apostolidos, B. Kanellakopulos, R. Maier, J. Rebizant and M. L. Ziegler, *J. Organomet. Chem.*, 1991, **409**, 243.
10 J. C. Green and C. N. Jardine, *J. Chem. Soc.*, *Dalton Trans.*, 1998, 1057.
11 S. Barlow, M. J. Drewitt, T. Dijkstra, J. C. Green, D. O'Hare, C. Wittingham, H. H. Wynn, D. P. Gates, I. Manners and J. K. Pudelski, *Organometallics*, 1998, **17**, 2113.
12 J. C. Green and A. Scottow, *New J. Chem.*, 1999, **23**, 651.
13 L. Fan and T. Ziegler, *J. Chem. Phys.*, 1991, **95**, 7401.
14 L. Lincoln and G. Wilkinson, *Inorg. Synth.*, 1980, **20**, 41.
15 I. E. Nifant'ev, P. V. Ivchenko and M. V. Borzov, *J. Chem. Res.* (*S*), 1992, 162.
16 N. J. Bailey, M. L. H. Green, M. A. Leech, J. F. Saunders and H. M. Tidswell, *J. Organomet. Chem.*, 1997, **538**, 111.
17 Z. Otwinowski, DENZO, Department of Molecular Biophysics and Biochemistry, Yale University, New Haven, CT, 1993.
18 Z. Otwinowski and W. Minor, *Methods Enzymol.*, 1996, 276.
19 D. J. Watkin, C. K. Prout, J. R. Carruthers and P. W. Betteridge, CRYSTALS, Issue 10, Chemical Crystallography Laboratory, University of Oxford, 1996.
20 D. J. Watkin, C. K. Prout and L. J. Pearce, CAMERON, Chemical Crystallography Laboratory, University of Oxford, 1996.
21 A. Altomare, G. Cascarano, C. Giacovazzo, A. Guagliardi, M. C. Burla, G. Polidori and M. Camalli, *J. Appl. Crystallogr.*, *Sect. A*, 1994, **27**, 435.
22 N. Walker and D. Stuart, *Acta Crystallogr.*, *Sect. A*, 1983, **39**, 158.
23 E. J. Baerends and G. te Velde, Department of Theoretical Chemistry, Vrije Universiteit, Amsterdam, 1997.
24 S. H. Vosko, L. Wilk and M. Nusair, *Can. J. Phys.*, 1980, **58**, 1200.
25 A. D. Becke, *Phys. Rev. A*, 1988, **38**, 2398.
26 J. P. Perdew, *Phys. Rev. B*, 1986, **33**, 8822.

Paper a908619f